Noname manuscript No.
(will be inserted by the editor)

Influence of Weight-on-Bit on Percussive Drilling Performance

Xianfeng Song · Ole Morten Aamo · Pascal-Alexandre Kane · Emmanuel Detournay

Received: date / Accepted: date

Abstract A phenomenological model for percussive drilling systems is proposed in this paper to explain the experimentally demonstrated existence of an optimal weight-on-bit (WOB), for which the rate of penetration (ROP) is maximized. Several hypotheses have been previously proposed to explain this universal characteristic of percussive drilling, including increased wear of the bit, reduced indexing, and poor cleaning of debris under excessive WOB. Motivated by experimental evidence, we instead consider an increase of the pseudo-stiffness of the bit-rock interface (BRI) with increasing WOB, and investigate its effect on the impact energy transmitted to the rock. The 1D model approximates the dynamics underlying the drilling process by assuming that the impact of the hammer generates a longitudinal wave in the bit. It is shown that the BRI pseudo-stiffness influences the incident wave and associated energy transmitted from the bit to the rock. As a consequence, the drilling efficiency is affected by the dependence of the BRI stiffness on the WOB. The model indicates that there exist optimal conditions for the energy transfer from the bit to the rock in terms of the impedance ratio and the BRI stiffness/WOB. Thus it confirms that there is a sweet spot as seen in practice, which suggests that the root cause of the existence of a sweet spot in the ROP-WOB relationship lies in the nature of the BRI laws, rather than with issues related to bit indexing, bit wear, and/or cleaning of the debris.

Keywords Percussive drilling · Weight-on-bit · Rate of penetration · Impact transmission efficiency

X. Song · O. Aamo
Norwegian University of Science and Technology, Trondheim, Norway

P. Kane
SINTEF Industry, Trondheim, Norway

E. Detournay
University of Minnesota, Minneapolis, USA
Tel.: +1-612-625-3043
Fax.: +1-612-626-7750
E-mail: detou001@.umn.edu

1 Introduction

A percussive drilling system, either a Top-Hammer (TH) or a Down-The-Hole (DTH) tool consists essentially of a pneumatically or hydraulically driven hammer and a bit assembly, see Fig. 1 for the schematic of a DTH tool. During the percussive drilling process, the hammering system converts the potential energy of the pressurized air or water into reciprocating movements of the hammer, which repeatedly impacts the bit assembly [1]. An impact induces a compressive incident wave that travels through the bit assembly to eventually cause penetration by indentation of a collection of bit buttons into the rock [2, 3].

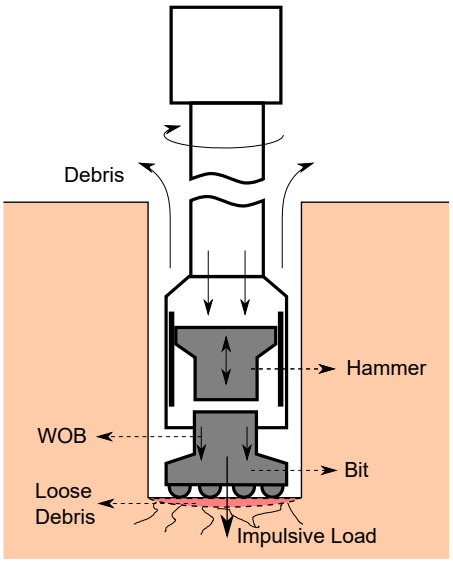

Fig. 1: Schematic of a DTH percussive drilling system.

Percussion tools are generally more efficient for drilling hard rock formations than conventional rotary equipment [4, 5]. Their advantages include lower weight-on-bit (WOB) requirement, reduced bit wear due to less contact time with the rock, less borehole deviation and larger chip size [6].

As with other mechanical excavation methods [7], rock breakage in percussion drilling results from penetration of an indenter into rock that causes crushing and the formation of tensile cracks. The produced rock cuttings are then flushed away from the rock surface by air or water. The rock fragmentation process is enhanced by the rotation of the drilling assembly, which causes the drill buttons to move between blows, with the subsequent impacts leading to the preferential development of lateral cracks [8]. Efficient transmission of the impact energy to the rock requires closing of the transient gap between the drill bit and rock surface before the next indentation; this is ensured by applying a sufficiently large thrust force (WOB) on the bit assembly.

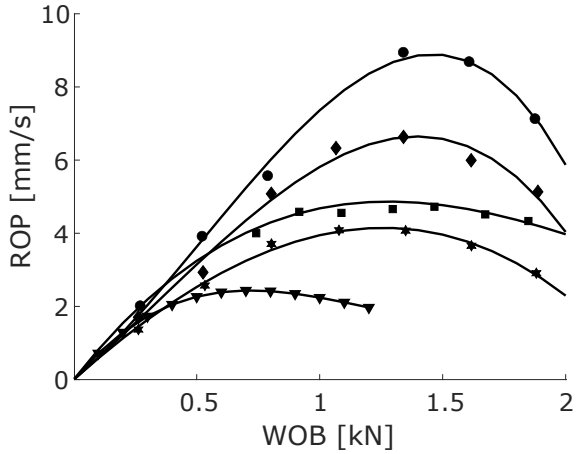

Fig. 2: Sweet spot in WOB-ROP response given different rock formations, pneumatic pressure, and bit types (adapted from [14, 16]). Symbol ▼ pertains to winged bit drilling of Pink Tennessee marble with a pneumatic pressure of 0.34MPa [14]; ●, ♦, ★ refer to winged bit, Swedish granite, and pneumatic pressure of 0.59MPa, 0.49MPa, 0.39MPa respectively [14]; ■ corresponds to button bit, Charcoal granite, and pneumatic pressure of 0.55MPa [16];

Although pneumatic percussive drilling has been in operation since the 1860's [7, 9], fundamental knowledge about the complex drilling process with such tools still remains somewhat elusive. The lack of understanding has limited the widespread application of this technique, in particular to the oil industry [10]. Specifically, there is no consensus regarding the root cause of the observed existence of an optimal state in the control variables. Indeed, many experiments have shown evidence that the average rate of penetration (ROP), the most important indicator for drilling performance, can be maximized for certain parameter sets, including the static WOB [1, 9, 11–14]. Such an optimal state is typically referred to as a "sweet spot" [15].

Laboratory and field data illustrated in Fig. 2 suggest that such an optimal configuration is a universal characteristic of percussive drilling, with the optimal WOB depending on several factors, such as rock formation, bit type, pneumatic pressure, and indexing angle. Nevertheless, a convincing explanation of the physics behind the existence of a sweet spot has not yet been proposed, in our opinion. Poor understanding of the root cause of this phenomenon is restricting the development of adaptive control algorithms to identify the sweet spot to strategies that are exclusively data-driven, without the benefits of insight provided by a mathematical model.

Various hypotheses have been advanced to explain the existence of a sweet spot: increased wear of the bit [17], reduced indexing (including stick-slip) [11, 18], and poor cleaning of the debris [19, 20]. These explanations, while perhaps applicable in particular cases, do not provide universal rationales, as a significant body of contradictory experimental evidence exists.

First a possible link between bit wear and the existence of a sweet spot is challenged by results of field experiments, where the bit was examined and sharpened periodically and wear can therefore be assumed to be negligible [9]. In any case, experiments show that bits with hemispherical buttons hold an exceptional resistance to abrasive wear [16]. Furthermore, in a series of tests, where the WOB was progressively increased, it was noted that moderate wear of the carbide inserts had already taken place during the ascending phase of the ROP versus WOB [21].

Decrease of ROP with increasing WOB beyond the optimum has been attributed to reduced indexing, presumably caused by the limited torque capacity of the equipment [18]. However, this explanation is contradicted by experimental results indicating that the specific energy for drilling granite with a button bit is essentially the same for three different indexing angles [16]. Furthermore, given a nearly constant rotation speed, Schunnesson [22] demonstrated that a higher ROP was obtained in a field test by reducing the WOB. Also, experiments conducted with different indexing angle [13] indicate that an optimum WOB exists irrespective of the indexing angle.

Finally, poor cleaning can generally be eliminated as a plausible cause to the existence of a sweet spot, since the flushing capacity of modern equipment (especially in laboratory experiments) is powerful enough to remove the debris efficiently.

Wiercigroch and co-workers [23–26] have studied the long-term dynamical response of drifting impact oscillators to explain the drop in ROP with increasing WOB in percussion drilling. Although the model is able to reproduce the optimal configurations observed in laboratory experiments, its direct applicability to percussive drilling is open to questions as it is framed in terms of rigid body dynamics rather than wave propagation and harmonic excitation is used to mimic percussive activation. Furthermore, an alternative drifting oscillator model based on a bilinear bit/rock interaction law and an impulsive rather than a harmonic loading could not reproduce an optimal configuration in the explored parametric range [27].

Instead, we propose a different mechanism behind the sweet spot and present the experimental evidence to support it. First we note that the timescales characterizing the percussion drilling processes span several orders of magnitude: $T_1 = O(10^{-2} \sim 10^{-1}s)$ is associated with the impact frequency of the hammer while $T_2 = O(\sim 10^{-4}s)$, corresponds to the pulse length of an impact and also measures the time duration of the bit penetration into the rock [15]. All the previous explanations for the existence of a sweet spot reviewed above actually involve the slow timescale. However, it is the fast process, responsible for the damage and the fracturing of the rock, that will eventually determine the drilling performance. Therefore, we propose to analyze the drilling process on the fast time scale. In a nutshell, the existence of the sweet spot can be explained by considering the force-penetration (F-P) curve during one impact. This response is strongly nonlinear, mainly due to the presence of a layer of loose rock debris and damaged rock between the drill bit and the intact rock. The interface layer is expected to exhibit a larger resistance to penetration during impact, i.e., a larger pseudo-stiffness, when subjected to a larger static WOB force.

Therefore, we consider an increase of the pseudo-stiffness of the BRI with the WOB and develop a phenomenological model to investigate its effect on the impact energy transmitted to the rock. According to the elastodynamic model, there exist optimal contact conditions for maximizing the energy transfer from the bit to the

rock in terms of the BRI pseudo-stiffness and the impedance ratio. A previous investigation by Hustrulid and Fairhurst [14] has already noted that an optimal loading slope of the F-P relation maximizes the energy transmission efficiency. Moreover, parametric studies conducted by Lundberg [28–30] also indicate the existence of an optimal hammer length, a function of the penetration resistance, for which the energy transmission efficiency is maximum. Nonetheless, the dependence of the pseudo-stiffness of the BRI on the WOB has not yet been suggested as an explanation for the observed dependance of the ROP on the WOB.

The paper is organized as follows. Section 2 reviews experimental evidence indicating that the observed WOB-ROP relationship actually reflects the non-monotonic relationship between the BRI pseudo-stiffness and the impact energy transmitted to the rock. Section 3 demonstrates with a 1D phenomenological model of percussion drilling that there is an optimal BRI pseudo-stiffness to maximize the energy transfer to the rock, provided that the bit impedance is small compared to the rock impedance. Section 4 supports the hypothesis that the impedance ratio between the bit and the rock is indeed small, on the basis of a finite element simulations and analysis of experimental data. Section 5 concludes that the root cause of the existence of a sweet spot in the ROP-WOB relationship indeed lies in the nature of the BRI laws.

2 Experimental Evidence

2.1 Preamble

Comprehensive research programs focused on percussion drilling of rock were conducted in the 1950's and 1960's at several research institutes, including the University of Minnesota [8, 13, 18, 31–39]. These efforts have provided valuable information on the influence of the WOB and of the damaged rock underneath the drill buttons on the drilling performance.

Two types of laboratory tests have been used in the research on percussion drilling: the drop test and the jackleg-type percussive drilling test. Despite the fundamental differences between the two tests in regard to the fraction of the impact energy used to drive the bit into the rock [40], the drop test is appealing because of its simplicity. Indeed the key factors influencing rock penetration can be assessed by adjusting the drop mass and geometry or the drop height and measuring the difference in the bit kinetic energy before and after impact, as well as the volume of the craters created by the impact. The main justification for using a drop test (DT) as a proxy to percussive drilling (PD) comes from the order of magnitude difference between the penetration time of the bit into the rock following an impact and the frequency of the hammer. In other words, the time elapsed between successive impacts is large enough that each penetration event can be considered to be independent regardless of the interactions between successive indentations [28, 33]. However, the usual drop tests cannot be used to characterize the influence the WOB on the drilling performance.

We review the experimental findings in light of our hypothesis that the dependence of the BRI pseudo-stiffness on the WOB is the key factor behind the existence of a sweet spot. In a nutshell, the experimental evidence indicates that

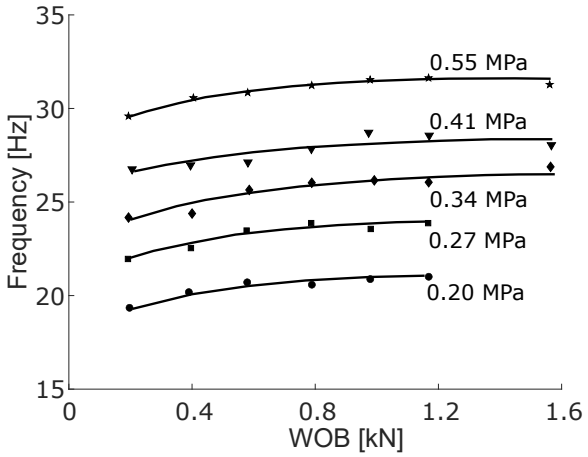

Fig. 3: Slightly increased frequency with WOB in the field percussive drilling tests, given different pneumatic pressure [18].

the pseudo-stiffness of the BRI increases with the WOB, and that the crater volume is proportional to the energy transmitted to the rock. These findings suggest to investigate the BRI stiffness impact on the energy transmission rather than directly evaluate the WOB-ROP relationship.

2.2 Energy dissipated in rock

2.2.1 Single percussive activation

The impact frequency of the hammer is observed to increase slightly with the applied WOB in percussive drilling tests [18], see Fig. 3; it is linked to a reduced hammer stroke [13]. Although the impact frequency slightly increases with harder rock, the mean raw hammer power (the product of the difference in the hammer kinetic energy before and after impact with the percussion frequency) remains constant for a given input pneumatic pressure [43]. In other words, the effective power delivered to the rock for fragmentation depends primarily on the energy transmission efficiency at each impact. Therefore, the assessment of the energy transmission can generally be performed by considering a single percussive activation.

2.2.2 Dissipated energy as a proxy for average bit penetration

Crater volumes caused by the bit impact in drop tests are found to be approximately proportional to the energy transferred to the BRI for a range of bit shapes, rock types, indexing angles and impact velocities [18], see Fig. 4. Thus the specific energy essentially remains constant in both static tests and drop tests irrespective of the drill bits used [31, 33, 35, 37, 38].

Through an averaging procedure, the mean bit penetration per impact can be viewed as being proportional to the energy dissipated in the rock. However,

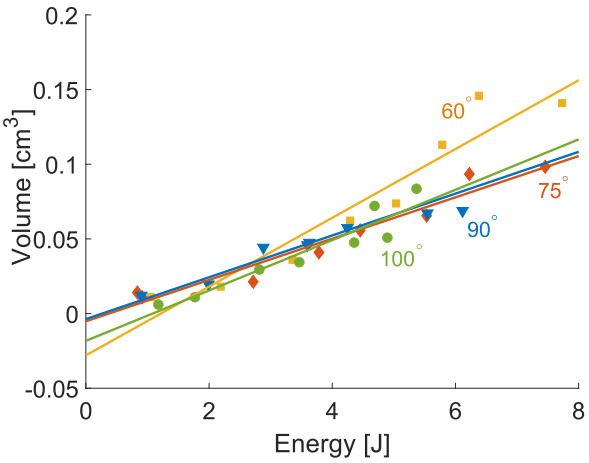

Fig. 4: Linear relationship between dissipated energy and crater volume for different apex angles (Conical bit and Georgia limestone), post-processing of data from [33].

an energy barrier is observed both in the static and dynamic test. Indeed, the energy transmitted to the rock below a threshold appears to cause very limited damage [18, 44]. Although a linear relationship between energy dissipated and mean bit penetration could in principle be questioned on the grounds that the bit impacts on a flat rock surface in drop tests might not truly represent actual drilling conditions, Hustrulid [18] and Haimson [31] have demonstrated that the effects of hole depth on the specific energy are negligible. Also, Lundquist [16] investigated the influence of the indexing angle on the penetration characteristics with button bits. For the three indexing angles (24°, 33°, 45°) used in his tests, little effect was observed on the specific energy after a few successive impacts.

The above evidence indicates that the factors influencing the ROP can be investigated by analyzing the energy transmission efficiency instead.

2.2.3 Rate effect

The question as to whether the specific energy and the F-P curve depend on the rate of loading has been addressed by many researchers, starting with pioneering work conducted in the 1950's by Drilling Research Incorporated (DRI). First note that the average impact velocity of the drill bit in percussive drilling is about $4 \sim 6$ m/s [31] and thus PD involves loading rates that are several orders of magnitude larger than those developed in quasi-static indentation.

Quasi-static indentation tests and drop tests performed by Hustrulid [18] revealed no significant differences in the F-P relationship and in the specific energy if the two test results are properly compared, see Fig. 5. It can also be seen from this figure that the first fracture/chipping in both tests occurred roughly at the same force level. Although it was later observed that the slope of a dynamic F-P curve for a smooth surface was about twice that of the static slope, the average

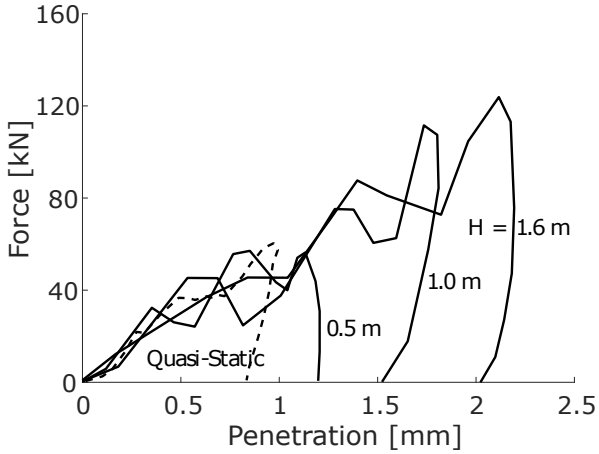

Fig. 5: Rate dependency characterization with winged bit penetrating Tennessee marble, where H represents different heights, post processed based on [18].

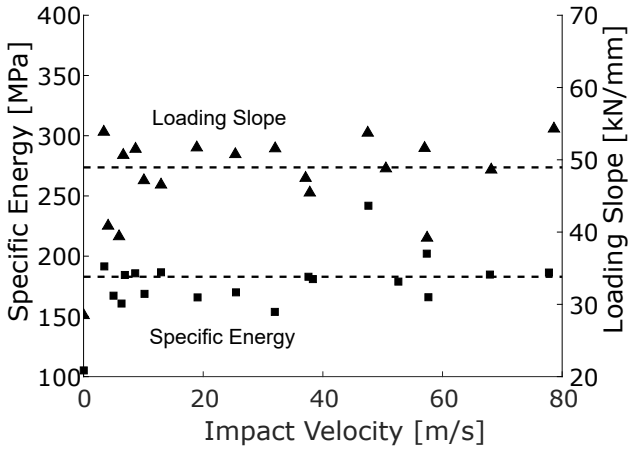

Fig. 6: No significant loading rate effect on specific energy and loading slope, after [31].

slopes on a rough surface are similar [45]. (The same peak force level was imposed in the two tests). Kou [7] further reported that a quasi-static approach provides reasonable damage predictions for velocities smaller than 160 m/s.

Haimson [31] employed a drop tester and a high-velocity apparatus to investigate the characteristics of bit-rock interaction for a wide range of impact velocities ($3 \sim 80$ m/s). Although the statically obtained slope of the F-P curve and the associated specific energy were considerably lower than in the dynamic test, no significant difference in the specific energy and average slope of F-P curve was observed over a large range of loading rates, see Fig. 6.

Investigations by Vanzant [46] of the effect of loading rate on the penetration of conical and sphere bullets in marble and cement were inconclusive, as different trends were observed for the two materials when analyzing the dependance of the crater volume on the bullet velocity.

Despite some conflicting experimental evidence, there is, however, general consensus that loading rate effects can be neglected in percussive drilling [19, 33, 34, 47–49]

2.3 Dependence of pseudo-stiffness on WOB

2.3.1 Increased BRI pseudo-stiffness with WOB

In percussive drilling tests conducted by Hustrulid [18] with an experimental set-up akin to a TH drill rig, the stress wave reflected from the BRI is observed to depend on the applied WOB levels. (The steel rod was designed to be long enough to prevent the interference of incident and reflected stress wave measurement.) At small WOB, the incident compressive stress wave essentially experiences a free-end reflection at the BRI, implying that virtually no energy is transmitted to the rock, refer to Fig. 7. As the WOB increases, the tensile portion of the wave becomes smaller while the compressive part becomes larger, which implies that the drill bit encounters more resistance at the BRI. Several more tests were implemented and superimposed to verify the repeatability of this observation [18]. It was found that the sequentially measured stress waves are identical given the same operating conditions, which also confirms the adequacy of focusing on a single impact, as done in this study.

In view of the nature of the set-up [18], the BRI of the F-P response can actually be determined from longitudinal wave theory given the measured incident and reflected stress wave, see Fig. 8. Our analysis of the experimental data indicates that the slopes of the F-P curves increase monotonically with the WOB, while the transmitted energy, which corresponds to the area under the F-P curve, increases with the WOB to reach a peak and then decreases. The presence of a small compressive portion occurring at the beginning of the reflected stress wave in Fig. 7 (refer to the red circle highlighted region) is considered to be caused by the increasing cross-sectional area at the bit front and not by the conditions at the BRI [18]. Hence, this effect is ignored when constructing Fig. 8, especially as only a slight difference is observed in a comparison of F-P curve with and without accounting for this small compressive portion.

2.3.2 Influence of rock damage on the BRI pseudo-stiffness

Repeated drop tests reveal a significant nonlinear F-P response characterized by increasing stiffness with penetration during the loading process, with the drill bit experiencing large displacement with relatively little resistance at the onset of penetration [2, 18], see Fig. 9. This nonlinear response is understood to be mainly caused by the rock damage formed by previous impacts. The presence of re-compacted fragments have a negative effect on the subsequent fragmentation process, although only a small amount of energy is absorbed by the re-compaction [50].

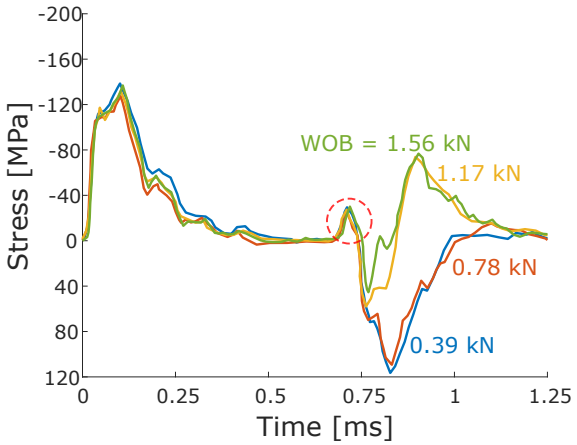

Fig. 7: WOB impact on the stress wave propagation, adapted from [18].

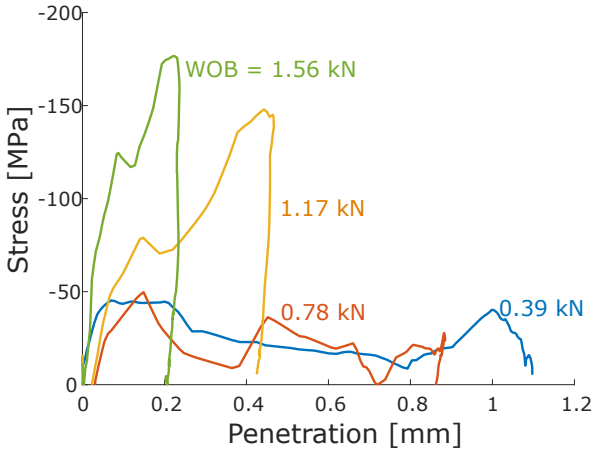

Fig. 8: WOB impact on the transmitted stress-penetration curve (post-processing based on data collected in [18]).

Considering that the loose debris thickness is about the same order of magnitude as the bit penetration after impact, it can be inferred that without application of a WOB, the incident stress is essentially reflected as from a free end before the bit can establish good contact with the intact rock. However, this loose fractured and damaged zone is recompacted and expected to exhibit a larger resistance to penetration during impact, when subjected to a larger static WOB force. This effect is revealed by a larger pseudo-stiffness.

For illustration purpose, a sketch of the damaged rock underneath the bit buttons is depicted in Fig. 10. In successive rings away from the indenter, one finds loose and partly compacted rock powder, crushed rock and fractured rock [7]. The

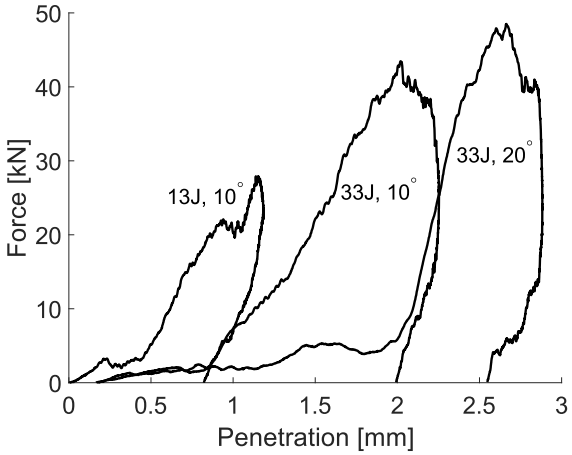

Fig. 9: Representative nonlinear force versus penetration curves obtained from drop tests for different impact energy and indexing angles, after [2].

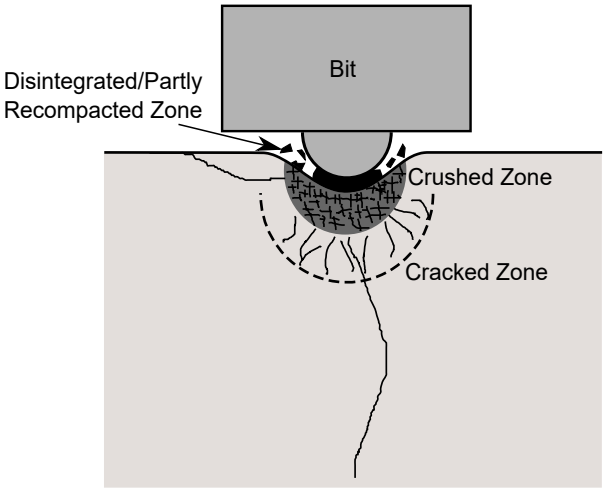

Fig. 10: Sketch of cracks in rocks under indentation [7].

size of the crushed and the fractured zone mainly depends on the magnitude of the loading, the rock macro-mechanical properties, and the geometry of the indenter [7]. In addition, three systems of cracks: median cracks, radial cracks and side cracks may exist outside the cracked zone.

2.4 Summary

The compiled experimental evidence leads to several remarkable results concerning the characteristics of percussive drilling.

1. The BRI law is rate-independent in the range of impact velocity involved in percussion drilling. It implies that the rate of penetration is proportional to the product of the impact frequency and the energy dissipated in rock fragmentation — essentially the energy transmitted to the rock — at each impact [51]. Since the percussion frequency varies little with the WOB and rock type given certain operating conditions, the transmitted energy per impact can be used as a proxy to the ROP to assess the influence of WOB.
2. The BRI law depends on the condition of the rock surface that is impacted by the bit. The presence of loose debris and subsurface damage lowers the apparent stiffness of the BRI, thus affecting the energy transmission and the maximum force that can be generated. The thickness of the damage zone is of the same order of magnitude as the bit displacement given a small WOB. This layer of damaged rock is known to respond non-linearly, with its normal stiffness increasing with the applied normal force.
3. The stiffness K of the interface increases with the WOB, as deduced from an analysis of the reflected stress wave in relation to the incident stress pulse generated by impact of the hammer. A relatively small WOB, however, is able to compact the loose debris to a large extent prior to the arrival of the impulsive load. Thus, the bit encounters higher resistance as penetration commences under a larger WOB.

In view of the experimental evidence that the BRI stiffness increases with the WOB and that any rate effects are negligible, it can be concluded that the influence of the WOB on the ROP can be investigated by analyzing the dependence of the energy transmitted to the rock as a function of the BRI pseudo-stiffness.

3 Force and Energy Transmitted to Rock at Each Impact

3.1 Conceptual Model

This extensive review of PD or DT experiments has led to the conclusion that the non-monotonic ROP-WOB relationship likely reflects the non-monotonic variation of the transmitted energy with the BRI pseudo-stiffness K. On this basis, we develop a simple one-dimensional model to evaluate the effect of K — a function of the WOB – on the stress wave/energy transmission efficiency of the percussive hammer system.

The model of the system consists of four collinear bodies, namely the hammer, the bit assembly in series with a spring representing the BRI and a dashpot to account for the intact rock, see the sketch in Fig. 11.

The hammer is treated here as a rigid mass m_h moving at velocity V_0 at the moment of impact [7]. Neglecting the wave propagation in the hammer is appropriate in view of the air-hammer geometry, which is usually designed to be a short cylinder with large diameter to attain sufficient impact velocities over a short stroke [52]. The accuracy of the rigid hammer approximation has been demonstrated by

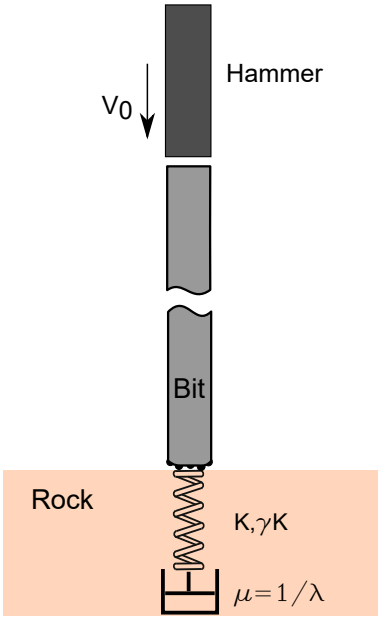

Fig. 11: 1D indentation model for percussive drilling.

Wu [52], who showed that the simulated incident wave presents little deviation from the measurement. For illustration purpose, a perfect contact is assumed at the hammer-bit interface (HBI) following the impact; the mismatch conditions due to the interface roughness are thus neglected. The HBI stiffness influence on the energy transmission efficiency has been investigated and demonstrated in [53].

The impact of the hammer on the bit at rest then induces stress waves propagating in the bit/BRI/rock system. The bit is regarded as an elastic cylinder with Young's modulus E. Since inertia effects in the rock being fractured is of small significance [54], a weightless spring is introduced at the BRI interface to represent the rock resistance to the bit penetration. Although a constant BRI loading pseudo-stiffness K is usually assumed in the literature, here motivated by experimental evidence, K is understood to increase with the WOB in this conceptual model. Furthermore, as we are mainly concerned by the maximum energy transmission during the penetrating phase, the unloading phase is simplified by assuming an abrupt drop of the F-P response after peak penetration. In this case, the unloading slope, γK, is assumed to be infinitely large, i.e., $\gamma \to \infty$. This simplification should be adequate, since it is usually observed that most of the bit penetration is irreversible as there is negligible recovery during unloading [55].

However, in the case of percussive drilling, reflection of incident wave occurs due to the discontinuity at the BRI. This discontinuity is partly attributed to the third-body formed by previous impact as discussed above and also the impedance mismatch between the bit and intact rock. From a mathematical point of view, the homogeneous intact rock can be approximated by a dashpot to account for the impedance contrast and the energy radiation effect.

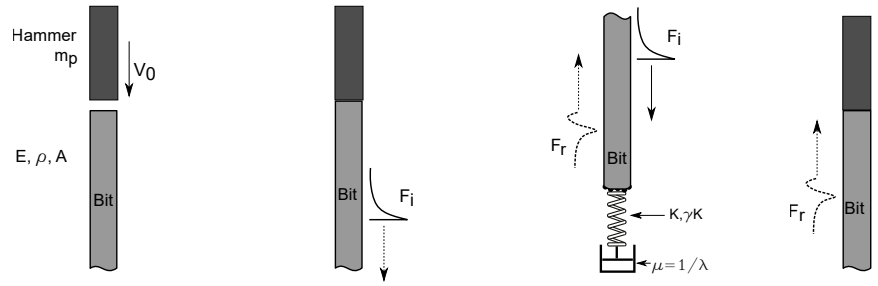

(a) Prior impact (b) Step 1 (c) Step 2 (d) Step 3

Fig. 12: Process for one cycle of wave production, propagation and reflection

Finally, we assume that each impact is independent on account that the time elapsed between two successive impacts is large enough [28, 33]. Indeed it is found that the dynamic stress in the bit assembly reduces to an insignificant level within 0.01 sec after impact, which is smaller than the time interval (about 0.03 sec, equivalent to a 30Hz hammering frequency) between two impacts [41]. The repetitiveness of the response to successive impact in percussive drilling tests, as indicated by the virtually identical strain waves, confirms the independence of each impact loading [18].

This simple 1D model can thus be used to explore the key factors influencing the energy and force transmission to the rock. It is motivated by the following considerations. First, the percussive drilling efficiency generally depends much more on the mass of the bit than on its shape [3], and the load magnitude is reported to be more important than its distribution across the face of the bit in the formation of subsurface fractures [7]. Second, the raw impact power delivered by the hammer to the bit-rock system remains essentially constant for a given input air pressure, despite the fact that WOB slightly changes the impact frequency [43]. The bit angular motion and the associated interaction among successive indentations are not considered in this analysis. Finally, wave attenuation and dispersion is not taken into account, considering that we only investigate the propagation of the first impulsive load. Hence the stress wave/energy is transmitted without any loss or distortion from the impacted end of the hammer to the BRI.

The stress perturbations can generally be interpreted as a sequence of three stages: (i) impact of the hammer on the bit, (ii) transmission of the stress wave through the BRI, and (iii) arrival of the reflected stress wave at the hammer/bit interface (HBI), see Fig. 12. Since we are interested in evaluating the stress/energy transmission during the first impulsive loading process, the last stage is ignored here.

3.2 First Stage: impact between hammer-bit

The impact of the rigid hammer on the bit provokes a longitudinal compressive force wave F_i propagating at speed c towards the BRI, as illustrated in Fig. 12b. The propagation of the elastic disturbance in the bit assembly is governed by the

longitudinal wave equation

$$\frac{\partial^2 U}{\partial t^2} = c^2 \frac{\partial^2 U}{\partial x^2} \tag{1}$$

where $U = U(x,t)$ represents the displacement of a particle x along the elastic rod as a function of time t. The longitudinal wave velocity $c = \sqrt{E/\rho}$, where E is Young's modulus and ρ is the density of the bit. d'Alembert's general solution resolves the wave equation by introducing a downward traveling wave U_i (traveling toward the BRI) and an upward traveling wave U_r (traveling away from the BRI)

$$U(x,t) = U_i(ct - x) + U_r\,(ct + x) \tag{2}$$

Initially, the solution is simply given by $U(x,t) = U_i(c_1 t - x)$ since there is no wave reflected from the BRI yet. The corresponding force $F(x,t)$ and particle velocity $V(x,t)$ distributed along the bit assembly is given by

$$F(x,t) = EA\frac{\partial U}{\partial x} = -EAU_i' \tag{3}$$

$$V(x,t) = \frac{\partial U}{\partial t} = cU_i' \tag{4}$$

where the prime denotes differentiation with respect to the argument of the function, and compression is taken to be negative. Thus before any arrival of the back reflected wave at this point, the particle velocity at x is simply proportional to the local incident force $V(x,t) = -\frac{F(x,t)c}{EA}$.

Provided the hammer impact on the drill bit is a momentum conservative process, the motion of the striking hammer can be solved according to the rigid body mechanics

$$m_h V_0 + \int_0^t F(0,\tau)\mathrm{d}\tau = m_h V_h(t) \tag{5}$$

with the origin of time taken to correspond to the moment of impact. In the above, $F(0,t)$ is the compressive force acting at the interface between the hammer and the bit, and $V_h\,(t)$ represents the hammer velocity at $t > 0$. As a consequence of assuming a rigid hammer and an ideal hammer-bit contact, there is an instantaneous jump of the force at the HBI after the impact, followed by an exponential decay [56]

$$F(0,t) = -\frac{EAV_0}{c}\exp\left(-\frac{EA}{m_h c}t\right) \tag{6}$$

where A refers to the uniform cross-sectional area of the bit, see Appendix A for details of the derivation. The impact force must be of a compressive nature, otherwise the two components are separated. In other words, the hammer cannot rebound but remain in contact with the bit, at least until the arrival of the wave reflected from the BRI.

In order to reduce the number of parameters in the expression, it is advantageous to reformulate the model in a dimensionless form by introducing scales. By nature, the percussive drilling process is characterized by multiple timescales [27]. Here in order to investigate the stress wave/energy transmission in one transmission cycle, the effective duration of the pulse generated by the impact of the hammer is selected as the time scale T_*; the hammer maximum movement following impact as the displacement scale U_*; the maximum impact force induced at

the HBI as the force scale F_*; and the hammer impact velocity as the velocity scale V_*. Thus,

$$T_* = \frac{m_h c}{EA} \quad U_* = \frac{m_h c V_0}{EA} \quad F_* = \frac{EAV_0}{c} \quad V_* = V_0 \tag{7}$$

Hence the dimensionless time τ, displacement u, force f, and dimensionless velocity v are defined as

$$\tau = \frac{t}{T_*} \qquad u = \frac{U}{U_*} \qquad f = \frac{F}{F_*} \qquad v = \frac{V}{V_*}$$

Therefore, prior to any reflected stress wave, the normalized force, displacement and velocity at the hammer-bit interface can be evaluated as

$$f(0,\tau) = -e^{-\tau}, \qquad u(0,\tau) = 1 - e^{-\tau}, \qquad v(0,\tau) = e^{-\tau} \tag{8}$$

Attenuation or dispersion during the incident wave propagation is assumed to be negligible before it reaches the BRI. Therefore, the non-dimensional incident force wave f_i at the BRI is identical to $f(0,\tau)$, but for a fixed time delay.

3.3 Second Stage: interaction beween bit and rock

In the second stage, the incident force wave f_i reaches the BRI, where it splits between a reflected wave denoted as f_r, and a transmitted wave f_t, which is responsible for the destructive work done on the rock, see Fig. 12c. The impact energy is essentially partitioned into three components: dissipation on rock fragmentation, elastodynamic radiation in the rock, and reflection to the hammer and the drill bit [54]. However, the energy radiated by elastic wave is small compared to the energy dissipated in rock fragmentation [54, 57, 58].

Numerous experiments have been conducted to characterize the F-P relationship at the BRI. The response of the interface consists of a loading phase at the end of which the bit reaches a maximum penetration. Indentation experiments generally show little rebound after reaching the maximum penetration [54, 59], which implies that virtually all the energy transferred through the BRI is dissipated and radiated, and limited energy is recovered from the rock. Therefore, in this study, we neglect the elastic recovery by assuming an abrupt drop of the force at the interface upon unloading.

With the origin of time reset to the instant when the incident wave arrives at the BRI, the incident wave at the BRI reads $f_i = -e^{-\tau}$. As derived in the Appendix, the transmitted force f_t during the loading process can be determined from the BRI law.

$$\frac{df_t}{d\tau} + \kappa\left(\lambda + 1\right) f_t = 2\kappa f_i, \quad 0 \le \tau \le \tau_p \tag{9}$$

where τ_p corresponds to the time instant when the loading process terminates. Accordingly, the transmitted force f_t in the loading phase is given by

$$f_t = 2\kappa \frac{e^{-\tau(\kappa+\kappa\lambda)} - e^{-\tau}}{\kappa + \kappa\lambda - 1} \tag{10}$$

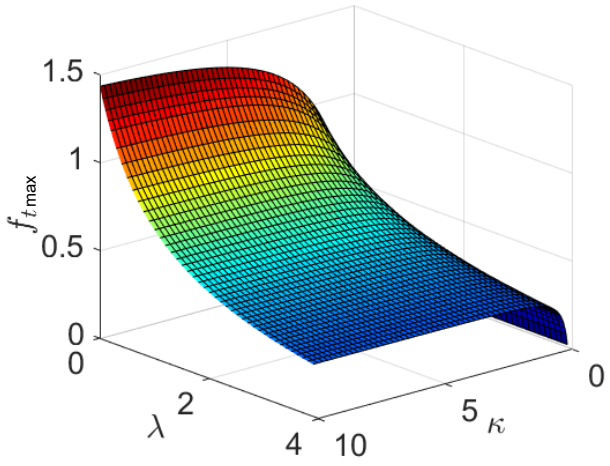

Fig. 13: Maximum transmitted force as a function of impedance ratio λ and BRI pseudo-stiffness κ.

Two numbers, κ and λ are introduced in the above equation: the scaled BRI pseudo-stiffness κ and the bit/rock impedance ratio λ

$$\kappa := \frac{K m_h c^2}{(EA)^2} \qquad \lambda := \frac{AE/c}{A_r E_r / c_r}. \tag{11}$$

The peak force $f_{t\,\max}$ transmitted at the BRI is reached at time τ_p when the penetration rate vanishes

$$\tau_p = \frac{\ln(\kappa + \kappa\lambda)}{\kappa + \kappa\lambda - 1}$$

and $f_{t\,\max}$ thus reads

$$f_{t\,\max} = \frac{2\kappa}{\kappa + \kappa\lambda - 1}\left((\kappa+\kappa\lambda)^{-\frac{\kappa+\kappa\lambda}{\kappa+\kappa\lambda-1}} - (\kappa+\kappa\lambda)^{-\frac{1}{\kappa+\kappa\lambda-1}}\right) \tag{12}$$

The dependence of the maximum force $f_{t\,\max}$ on the BRI pseudo-stiffness κ and on the impedance ratio λ is illustrated in Fig. 13. This figure shows that $f_{t\,\max}$ increases asymptotically with κ but decreases with λ. This latter trend is in agreement with experimental observations that the maximum transmitted force increases as the rock becomes stiffer [54]. The maximum force $f_{t\,\max}$ ultimately saturates around 2 as $\lambda \to 0$, $\kappa \to \infty$, which is analogous to a reflection from a fixed boundary. At this limit, the force transmitted at the BRI is twice the incident force.

A portion of the incident stress wave is reflected from the BRI and travels backward to the hammer-bit interface. The reflected force, denoted as f_r, is given by

$$f_r = \frac{2\kappa e^{-\tau(\kappa+\kappa\lambda)}}{\kappa + \kappa\lambda - 1} + e^{-\tau} - \frac{2\kappa e^{-\tau}}{\kappa + \kappa\lambda - 1} \tag{13}$$

In general, the reflected stress wave consists of an initial tensile portion following by a compressive tail. The impact loading phase prevails as long as the bit penetration proceeds. Once the maximum penetration has been reached, the unloading phase occurs along the idealized vertical F-P curve. Hence, the transmitted force during the unloading phase is determined as:

$$f_t = \frac{2f_i}{1+\lambda}$$

Accordingly, the work w_t expended by the transmitted force f_t on the rock is

$$w_t = \int_0^{\tau_i} f_t v_b d\tau \tag{14}$$

where τ_i is the incident impulse length which determines the duration for the wave transmission, and v_b is the bit bottom-end velocity given by $v_b = f_r - f_i$. Note that the work done by the static WOB during penetration of the bit is very small compared to the energy dissipated on rock fragmentation [43, 44], and is therefore neglected.

3.4 Efficiency

Both the experimental evidence and the numerical simulations summarized in the next Section suggest that the impedance ratio λ is small. Therefore, the condition $\lambda = 0$ is a useful limiting case to investigate the conditions leading to the maximum energy transfer in percussive drilling. Let $\eta\,(= 2w_t)$ denote the proportion of the impact energy that is transmitted to the rock during the first wave propagation cycle (in the absence of multiple reflections). In the limiting case, $\lambda = 0$, which implies a rigid rock foundation, and $\gamma \to \infty$, the energy transmission efficiency is given by

$$\eta = \frac{4\kappa}{(\kappa-1)^2}\left(\kappa^{1/1-\kappa} - \kappa^{\kappa/1-\kappa}\right)^2 \tag{15}$$

The dependence of η on κ is plotted in Fig. 14. The plot of $\eta\,(\kappa)$ indicates that $\eta \to 0$ in the two limits when either $\kappa \to 0$ or $\kappa \to \infty$ and that the transmission efficiency is maximum at $\kappa = 1$ with $\eta_{\max} = 4e^{-2} \simeq 0.54$.

No energy is transmitted to the rock by the incident wave if the BRI pseudo-stiffness $\kappa = 0$, which reflects a situation where the BRI offers negligible resistance to the bit advance. The small κ regime is in agreement with Hustrulid's observation [18] that the incident stress wave was reflected as from a free end under a small WOB and the net work (corresponding to the area under the F-P curve) is approximately zero. Moreover, if the BRI pseudo-stiffness $\kappa \to \infty$, $\lambda = 0$, which essentially represents fixed end condition, no energy will be transferred to the rock either, since no displacement is produced at BRI. Therefore, there must exist an optimal condition for the energy transfer from the bit to the rock (interpreted as the ROP) in terms of the BRI pseudo-stiffness (which is monotonically dependent on the WOB).

The more general conditions when the impedance ratio is non-zero is illustrated in Fig. 15. This figure, which plots the variation of the energy transmission efficiency with both κ and λ, shows that there is an optimal BRI stiffness, function

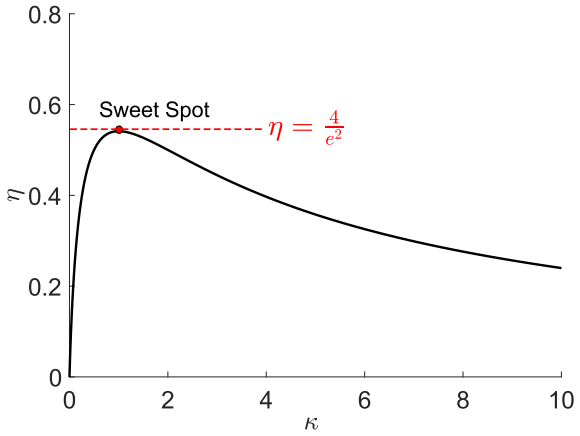

Fig. 14: Variation of energy transmission efficiency η with BRI stiffness κ. The maximum efficiency, $4e^{-2}$, corresponds to $\kappa = 1$ for $\lambda = 0$.

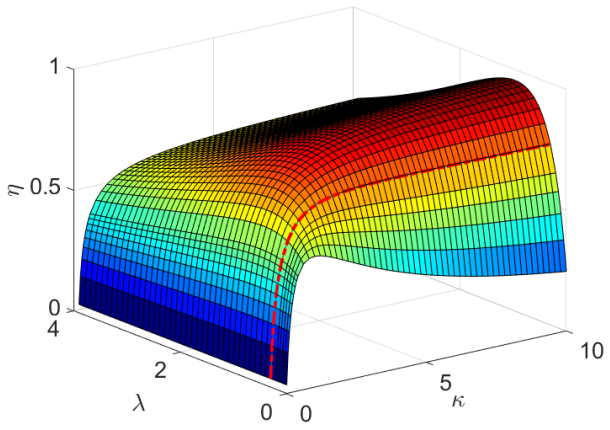

Fig. 15: Energy transmission efficiency in terms of pseudo-stiffness κ and impedance ratio λ.

of impedance ratio, that maximizes the energy delivered from the bit to the rock, provided that λ is small enough. For λ larger than the estimated critical value λ_*=0.3, the existence of an optimum κ disappears. In particular, the transmission efficiency η increases asymptotically with κ from 0 to 1 when $\lambda = 1$ suggesting that all the impact energy can theoretically be transferred through the BRI provided a good contact and the same impedance between the bit and intact rock. The incident wave and impact energy are fully reflected in the limit of an infinite impedance ratio.

In summary, the 1D phenomenological model shows that the BRI pseudo-stiffness κ and the bit-rock impedance ratio λ are the two critical numbers determining the drilling performance. There exists an optimal stiffness κ, which maximizes the energy transmitted from the bit to the rock, provided that the impedance ratio is small enough.

4 Discussion

According to the 1D phenomenological model described in this paper, the existence of a sweet spot hinges on the smallness of the impedance ratio. We demonstrate the plausibility of a small λ in percussion drilling by interpreting experimental data and also by estimating λ from numerical simulations conducted with an axisymmetric finite element model. Calculations performed for various values of the interface stiffness also confirm the existence of a sweet spot.

4.1 Estimate of impedance ratio from test data

A set of data from a published laboratory percussion drilling experiment [52] provides an opportunity to estimate the actual impedance ratio λ. In this particular experiment, the incident force wave essentially experiences a fixed-end reflection, as the amplitude of reflection is approximately the same as the incident wave and the tensile portion is almost negligible [54]. Such a signature is only possible if κ is sufficiently large (so that the BRI is effectively characterized only by an impedance contrast) and λ is small. According to longitudinal wave considerations about the transmission and reflection of an incident wave across a material discontinuity, λ can be assessed from

$$\lambda = \frac{f_i - f_r}{f_i + f_r} \tag{16}$$

Alternatively, Eq. (16) can be deduced from Eq. (9) by noting that bounded term $\frac{df_t}{d\tau}$ disappears for large κ. However, the mean value of λ is better estimated from

$$\int_0^{\tau_p} \lambda^2 d\tau = \int_0^{\tau_p} \frac{f_i^2 + f_r^2 - 2f_i f_r}{f_i^2 + f_r^2 + 2f_i f_r} d\tau$$

where the duration of loading phase τ_p is estimated from the drilling data. For the experiments reported by [52], the average λ is estimated to be 0.13.

There is also indirect evidence that more impact energy is absorbed by less competent rock in percussive drilling tests [54]. Interpreting these observations within the framework of the model, these observations indicate that the energy transmission efficiency increases with λ, which is inversely proportional to the rock elastic modulus according to Eq. (11). However, such a trend is only possible if λ is small, as can be seen in Fig. 16, where the range of λ is restricted to a small range. In this range of λ, an optimal pseudo-stiffness likely exists for maximizing the energy transmission.

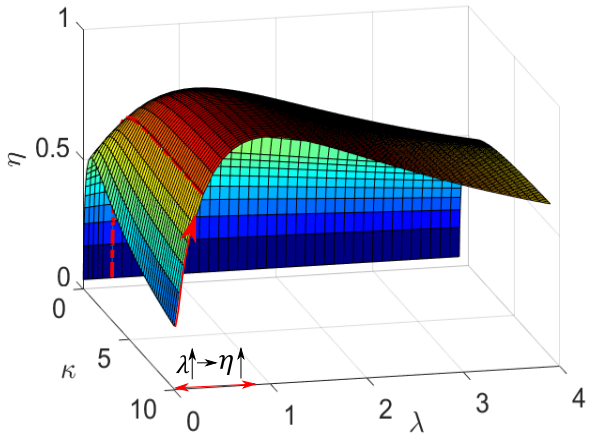

Fig. 16: Energy transmission effficiency plot in terms of pseudo-stiffness and impedance ratio, from a different angle.

4.2 Estimate of Impedance Ratio from Simulation

The impedance ratio λ can also be estimated from numerical simulations with the rock mass represented by a 3D elastic continuum. Here we report the results of numerical simulations showing that the impedance ratio is small (see Fig. 17).

The axisymmetric model used for the simulations is developed in COMSOL Multi-physics. For simplicity, the bit assembly is modeled as a cylinder, and all the bit buttons are replaced by an equivalent rigid button. The inertial effect of the third body is neglected by assuming its density to be zero. In addition, the Poisson ratio for the third body and the drill bit is assumed to be zero to mimic the spring resistance effect and wave propagation in a bar as in the one-dimensional model. Besides, in order to conveniently characterize the effect of the impedance ratio on impact transmission, the BRI pseudo-stiffness influence on the stress wave/energy transmission is eliminated by assuming a large Young's modulus of the third-body. Finally, the non-reflective boundary condition is imposed at the lower and outer boundary of the rock to mimic the semi-infinite nature of the rock mass.

A high quality mesh consisting of triangular and quadrilateral elements was generated by applying COMSOL default mesh function "free triangular" and "mapped mesh" on the rock and on the bit domain, respectively. A high resolution mesh is defined in the vicinity of the BRI to accurately capture the penetration and force transmission. The rock was discretized with 3002 elements, the third body with 40, and the drill bit assembly with 4656. A pre-defined incident force wave was applied on the upper bound of the drill bit assembly: $F_i = (F_* t/T_*) \exp(-t/T_*)$, where $T_* = 2 \cdot 10^{-5}$[s] and $F_* = 2 \cdot 10^5$ [N]. The total simulation time was $8 \cdot 10^{-4}$ s, with the integration time step set to 10^{-8}. The material properties and geometry details are given in Table 1.

Components	E (GPa)	ν	ρ (kg/m^3)	Dimensions (cm)
Bit	200	0	7800	H: 199, W: 2
Button	890	0.07	3510	H: 1, W: 0.6
Third Body	1000	0	0	H: 1, W: 3
Rock	60	0.2	2707	H: 299, W: ∼100

Table 1: Parameters used in the FE analysis: Young's modulus E, Poisson's ratio ν, density ρ, and dimensions of height H and width W.

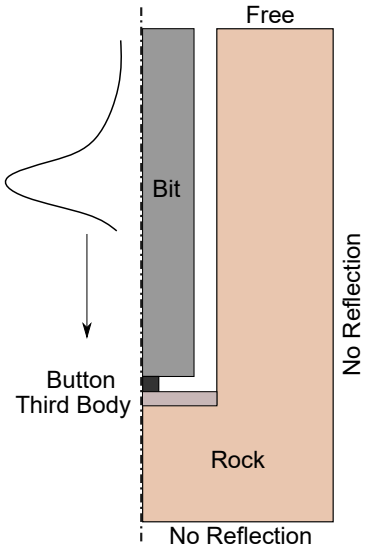

Fig. 17: Geometry built in the FEA analysis.

The impedance ratio λ was directly calculated from

$$\lambda = -\frac{v_b}{f_t} \tag{17}$$

where the velocity v_b of the button bottom and the transmitted force f_t can be extracted directly during the simulation. It is estimated the average impedance ratio in this numerical model is less than 0.1.

4.3 Simulation of Sweet Spot

The influence of the BRI pseudo-stiffness on the stress wave/energy transmission was investigated with the FE model by conducting a parametric study of the third-body stiffness, see Fig. 17. The simulations confirm that that an optimal pseudo-stiffness exists for maximizing the energy transmission, see Fig. 18. This optimal configuration appears regardless of the yield criterion, either Drucker-Prager or Hoek-Brown, to simulate failure of the rock under the button.

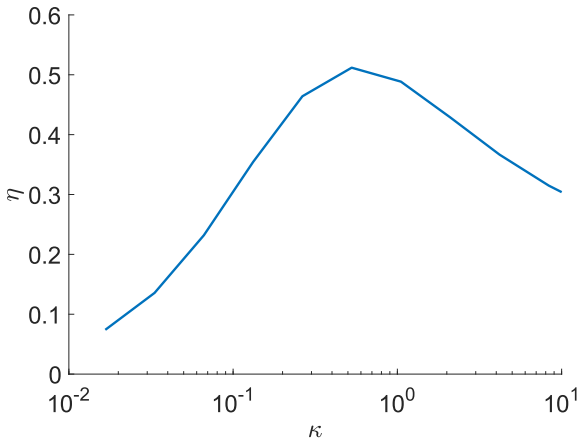

Fig. 18: Variation of the energy transmission efficiency η with the BRI pseudo-stiffness, as computed with the FE model.

5 Conclusions

The phenomenological model for percussion drilling described in this paper predicts a non-monotonic dependence of the transferred energy on the BRI pseudo-stiffness and thus the existence of an optimum WOB that maximizes the ROP – the so-called sweet spot. According to this model, the root cause behind the sweet spot is the dependence of the BRI pseudo-stiffness on the WOB. This explanation contrasts with the various reasons advanced in the literature, which include increasing wear of the bit, reduced indexing, and poor cleaning of the debris. A review of the published experimental data has uncovered evidence that the ROP is directly related to energy transmitted to the rock at each impact, and that the BRI pseudo-stiffness increases with the WOB. Moreover, a simple 1D model shows that there is an optimal BRI pseudo-stiffness that maximizes energy transmission to the rock during the first impulsive wave, provided that the bit/rock impedance ratio is small. With further enhancements, this model can form the basis for a model-based parameter identification and ROP optimization control algorithm running in real-time alongside the drilling operation.

Acknowledgement

This study is a part of the research project INNO-Drill (Technology platform for research-based innovations in deep geothermal drilling) funded by The Research Council of Norway (grant 254984) and industry partners (Epiroc, Enel Green Power, Lyng Drilling, NOV, Ravel, Robit, Rock Energy, Sandvik Mining and Construction, Tomax and Zaptec).

References

1. R. Ghosh, H. Schunnesson, A. Gustafson, Monitoring of Drill System Behavior for Water-Powered In-The-Hole (ITH) Drilling, Minerals **7**(7), 121 (2017). DOI 10.3390/min7070121
2. M. Fourmeau, A. Depouhon, A. Kane, H. Hoang, E. Detournay, Influence of indexation and impact energy on bit/rock interface law in percussive drilling: An experimental study, in *49th U.S. Rock Mechanics/Geomechanics Symposium* (American Rock Mechanics Association, San Francisco, California, 2015)
3. B. Lundberg, Microcomputer simulation of stress wave energy transfer to rock in percussive drilling, International Journal of Rock Mechanics and Mining Sciences & Geomechanics Abstracts **19**(5), 229 (1982). DOI https://doi.org/10.1016/0148-9062(82)90221-2
4. L.F.P. Franca, A bit–rock interaction model for rotary–percussive drilling, International Journal of Rock Mechanics and Mining Sciences **48**(5), 827 (2011). DOI 10.1016/j.ijrmms.2011.05.007
5. G. Han, M.B. Dusseault, E. Detournay, B.J. Thomson, K. Zacny, *Principles of Drilling and Excavation* (John Wiley & Sons, Ltd, 2009), chap. 2, pp. 31–140. DOI 10.1002/9783527626625.ch2
6. M.S. Bruno, Fundamental Research on Percussion Drilling : Improved rock mechanics analysis , advanced simulation technology , and full- scale laboratory investigations. Tech. Rep. 626, Terralog Technologies Inc (2005)
7. S. Kou, Some Basic Problems in Rock Breakage by Blasting and by Indentation. Ph.D. thesis, Tekniska Högskolan i Luleå (1995)
8. H.L. Hartman, The Effectiveness of Indexing in Percussion and Rotary Drilling, International Journal of Rock Mechanics & Mining Sciences **3**, 265 (1966)
9. A. Muhammad, Control of ith percussive long hole drilling in hard rock. Ph.D. thesis, McGill University (1996)
10. G. Han, M. Bruno, K. Lao, Percussion Drilling in Oil Industry : Review and Rock Failure Modelling, in *AADE 2005 National Technical Conference and Exhibition* (Houston, Texas, 2005)
11. S. Kivade, C.S. Murthy, H. Vardhan, Experimental Investigations on Penetration Rate of Percussive Drill, Procedia Earth and Planetary Science **11**, 89 (2015). DOI 10.1016/j.proeps.2015.06.012
12. H.F. Unger, R.R. Fumanti, Percussive drilling with independent rotation, U.S. Dept. of Interior, Bureau of Mines (1972)
13. E. Cheetham, WR and Inett, Factors affecting the performance of percussive drills, Transactions of the Institution of Mining and Metallurgical Engineers **63**, 45 (1953)
14. W.A. Hustrulid, C. Fairhurst, A theoretical and experimental study of the percussive drilling of rock Part IV-application of the model to actual percussion drilling, International Journal of Rock Mechanics and Mining Sciences & Geomechanics Abstracts **9**(3), 431 (1972). DOI https://doi.org/10.1016/0148-9062(72)90007-1
15. A. Depouhon, Integrated dynamical models of down-the-hole percussive drilling. Ph.D. thesis, Université de Liège, Liège, Belgique (2014)
16. R.G. Lundquist, Rock drilling characteristics of hemispherical insert bits. Master's thesis, University of Minnesota (1968)

17. E. Nordlund, The effect of thrust on the performance of percussive rock drills, International Journal of Rock Mechanics and Mining Sciences & Geomechanics Abstracts **26**(1), 51 (1989). DOI https://doi.org/10.1016/0148-9062(89)90525-1
18. W.A. Hustrulid, A study of energy transfer to rock and prediction of drilling rates in percussive drilling. Master's thesis, University of Minnesota (1965)
19. W. C. Maurer, The "Perfect - Cleaning" Theory of Rotary Drilling, Journal of Petroleum Technology **14**, 1270 (1962). DOI 10.2118/408-PA
20. G. Pearse, Hydraulic Rock Drills, Minning Magzines pp. 220–231 (1985)
21. S. Shaw, Effects of Farying Degrees of Rotation on Rate of Penetration of Percussion Drill Bits, Unpublished Report (1965)
22. H. Schunnesson, Drill Process Monitoring in Percussive Drilling-A Multivariate Approach To Data Analysis. Ph.D. thesis, Luleå University of Technology (1990)
23. A.M. Krivtsov, M. Wiercigroch, Penetration rate prediction for percussive drilling via dry friction model, Chaos, Solitons & Fractals **11**(15), 2479 (2000)
24. E. Pavlovskaia, M. Wiercigroch, C. Grebogi, Modeling of an impact system with a drift, Physical Review E **64**(5), 056224 (2001)
25. O.K. Ajibose, M. Wiercigroch, E. Pavlovskaia, A.R. Akisanya, Global and local dynamics of drifting oscillator for different contact force models, International Journal of Non-Linear Mechanics **45**(9), 850 (2010)
26. O.K. Ajibose, M. Wiercigroch, E. Pavlovskaia, A.R. Akisanya, G. Károlyi, Drifting impact oscillator with a new model of the progression phase, Journal of applied mechanics **79**(6) (2012)
27. A. Depouhon, V. Denoël, E. Detournay, Numerical simulation of percussive drilling, International Journal for Numerical and Analytical Methods in Geomechanics **39**(8), 889 (2015). DOI 10.1002/nag.2344
28. B. Lundberg, Energy transfer in percussive rock destruction-I: Comparison of percussive methods, International Journal of Rock Mechanics and Mining Sciences & Geomechanics Abstracts **10**(5), 381 (1973). DOI 10.1016/0148-9062(73)90024-7
29. B. Lundberg, Microcomputer simulation of percussive drilling, International Journal of Rock Mechanics and Mining Sciences & Geomechanics Abstracts **22**(4), 237 (1985). DOI 10.1016/0148-9062(85)92951-1
30. B. Lundberg, M. Okrouhlik, Influence of 3D effects on the efficiency of percussive rock drilling, International Journal of Impact Engineering **25**(4), 345 (2001). DOI 10.1016/S0734-743X(00)00053-1
31. B. Haimson, High velocity, low velocity and static bit penetration characteristics in Tennessee Marble. Master's thesis, University of Minnesota (1966)
32. J. Paone, D. Madson, W.E. Bruce, U. States., B. of Mines., *Drillability studies-laboratory percussive drilling* (U.S. Dept. of the Interior, Bureau of Mines, [Washington, D.C.], 1969)
33. C. W. Berry, Effect of Varying Bit Shape on Force-Penetration Characteristics in Rock for Impulsive Loading. Master's thesis, University of Minnesota (1959)
34. H.L. Hartman, Basic studies of percussion drilling, Mining Engineering **11**, 68 (1959)
35. C. W. Maurer, Impact crater formation in sandstone and granite. Master's thesis, Colorado School of Mines (1959)

36. P.F. Gnirk, An experimental investigation of the indexing phenomenon for static single-tooth penetration in Indiana limestone, University of Minnesota School of Mines and Metallurgy (1962)
37. H. Hartman, Crater geometry relations in percussive drilling, Mine and Quarry Engineering (1962)
38. B.R. Stephenson, Measurement of Dynamic Force-Penetration Characteristics in Indiana Limestone. Master's thesis, University of Minnesota (1963)
39. R. Simon, Transfer of the stress wave energy in the drill steel of a percussive drill to the rock, International Journal of Rock Mechanics and Mining Sciences & Geomechanics Abstracts **1**(3), 397 (1964). DOI 10.1016/0148-9062(64)90006-3
40. X. Song, P.A. Kane, O.M. Aamo, E. Detournay, A time scale regard on percussion drilling, International Journal of Impact Engineering (2020). Submitted, June 2020
41. G. Han, M. Bruno, Lab investigations of percussion drilling from single impact to full scale fluid hammer, in *41st US Rock Mechanics/Geomechanics Symposium* (American Rock Mechanics Association, Golden, Colorado, 2006)
42. W.A. Hustrulid, C. Fairhurst, A theoretical and experimental study of the percussive drilling of rock part III-experimental verification of the mathematical theory, International Journal of Rock Mechanics and Mining Sciences and **9**(3), 417 (1972). DOI 10.1016/0148-9062(72)90006-X
43. L.E. Izquierdo, L.E. Chiang, A methodology for estimation of the specific rock energy index using corrected down-the-hole drill monitoring data, Mining Technology **113**(4), 225 (2004). DOI 10.1179/037178404225006218
44. D. Zou, Rock Drilling, in *Theory and Technology of Rock Excavation for Civil Engineering* (Springer, Singapore, 2017), pp. 49–103. DOI 10.1007/978-981-10-1989-0
45. W.A. Hustrulid, Theoretical and experimental study of percussive drilling of rock. Ph.D. thesis, University of Minnesota (1968)
46. B.W. Vanzant, Dynamic rock penetration tests at atmospheric pressure, in *5th Symposium on rock Mechanics* (University of Minnesota, 1962)
47. R. Worsley, Energy, impulse, and velocity effects in fracturing produced by chisel bits in limestone. Ph.D. thesis, Colorado School of Mines (1960)
48. C. Fairhurst, Wave Mechanics of Percussive Drilling, Mine and Quarry Engineering pp. 122–130 (1961)
49. C.D. Haynes, Constant energy-variable velocity effects in percussive drilling. Ph.D. thesis, Pennsylvania State University (1963)
50. P.A. Lindqvist, L. Hai-hui, Behaviour of the Crushed Zone in Rock Indentation, Rock Mechanics and Rock Engineering **207**, 199 (1983)
51. Howard L. Hartman, Drilling Principles, in *Surface Mining, 2nd Edition*, ed. by B.A. Kennedy, B. A. Kennedy (Society for Mining, Metallurgy, and Exploration, 1990), chap. Mining Ope, pp. 513–523
52. C. Wu, Influence of Springy Impact Interface and Curved Drill Rods on Energy Transfer in Percussive Rock Drilling. Ph.D. thesis, Luleå University of Technology (1993)
53. C. Wu, An analytical study of percussive energy transfer in hydraulic rock drills, Mining Science and Technology **13**(1), 57 (1991). DOI 10.1016/0167-9031(91)90254-A

54. L.E. Chiang, D.A. Elías, Modeling impact in down-the-hole rock drilling, International Journal of Rock Mechanics and Mining Sciences **37**(4), 599 (2000). DOI 10.1016/S1365-1609(99)00124-0
55. B. Lundberg, P. Collet, Optimal wave with respect to efficiency in percussive drilling with integral drill steel, International Journal of Impact Engineering **37**(8), 901 (2010). DOI 10.1016/J.IJIMPENG.2010.02.001
56. K.F. Graff, *Wave Motion in Elastic Solids*. Dover Books on Physics Series (Dover Publications, 1975)
57. R. Simon, Energy Balance in Rock Drilling, in *Texas Drilling and Rock Mechamcs Symposium* (Society of Petroleum Engineers, 1963). DOI 10.2118/499-PA
58. B. Lundberg, M. Okrouhlik, Efficiency of a percussive rock drilling process with consideration of wave energy radiation into the rock, International Journal of Impact Engineering **32**(10), 1573 (2006). DOI 10.1016/J.IJIMPENG.2005.02.001
59. W.A. Hustrulid, C. Fairhurst, A theoretical and experimental study of the percussive drilling of rock Part II-force-penetration and specific energy determinations, International Journal of Rock Mechanics and Mining Sciences & Geomechanics Abstracts **8**(4), 335 (1971). DOI https://doi.org/10.1016/0148-9062(71)90046-5

A Appendix

A.1 Hammer-Bit Interface

The equation governing the evolution of the displacement of the HBI following impact is formulated by substituting into Eq. (5), the following expressions for the velocity and force at the HBI

$$V_h(t) = \frac{\partial U}{\partial t}\,|_{x=0} = cU'(ct) \tag{18}$$

$$F(0,t) = EA\frac{\partial U}{\partial x}\,|_{x=0} = -EAU'(ct) \tag{19}$$

which are obtained by setting $x = 0$ in Eqs. (3) and (4). Thus

$$\int_0^t U'(c\tau)d\tau = -\frac{m_h}{EA}\left(cU'(ct) - V_0\right) \tag{20}$$

After integrating the left term, this equation becomes

$$U'(ct) + \frac{EA}{m_h c^2}U(ct) = \frac{EA}{m_h c^2}U(0) + \frac{V_0}{c} \tag{21}$$

whose general solution is

$$U(ct) = De^{-\frac{EA}{m_h c}t} + U(0) + \frac{m_h c}{EA}V_0 \tag{22}$$

After identifying the constant D using the initial condition $U(0) = 0$, the displacement of the HBI induced by the impact of the rigid hammer is is given by

$$U(ct) = \frac{m_h c V_0}{EA}\left[1 - e^{-\frac{EA}{m_h c}t}\right] \tag{23}$$

The displacement increases from $t = 0$ to asympotically reach $\frac{m_h c V_0}{EA}$ at large time provided that the elastic bit assembly is unbounded.

A.2 Bit-Rock Interface

Once the incident wave reaches the BRI, the force balance at the interface is given by

$$f_t = \kappa(u_2 - u_1),\ 0 \le \tau \le \tau_p \tag{24}$$

where u_1 and u_2 represent the displacement at the BRI on the bit and rock side, respectively. Differentiating Eq. (24) with respect to time yields

$$\frac{df_t}{d\tau} = \kappa(v_2 - v_1), 0 \le \tau \le \tau_p \tag{25}$$

Given the assumed semi-infinite and homogeneous nature of the rock, no wave reflection in the rock will occur. Hence, the velocity v_1 and v_2 on both sides of the interface can be expressed as

$$\begin{cases} v_1 = f_t - 2f_i \\ v_2 = -\lambda f_t \end{cases}, 0 \le \tau \le \tau_p \tag{26}$$

Substituting Eq. (26) back into Eq. (25) yields the equation governing the evolution of the force applied by the bit on the rock

$$\frac{df_t}{d\tau} + \kappa\left(\lambda + 1\right) f_t = 2\kappa f_i,\ 0 \le \tau \le \tau_p \tag{27}$$